BIODIVERSITY

Genetic diversity loss in the Anthropocene

Moises Exposito-Alonso[1,2,3]*, Tom R. Booker[4,5], Lucas Czech[1], Lauren Gillespie[1,6], Shannon Hateley[1], Christopher C. Kyriazis[7], Patricia L. M. Lang[2], Laura Leventhal[1,2], David Nogues-Bravo[8], Veronica Pagowski[2], Megan Ruffley[1], Jeffrey P. Spence[9], Sebastian E. Toro Arana[1,2], Clemens L. Weiß[9], Erin Zess[1]

Anthropogenic habitat loss and climate change are reducing species' geographic ranges, increasing extinction risk and losses of species' genetic diversity. Although preserving genetic diversity is key to maintaining species' adaptability, we lack predictive tools and global estimates of genetic diversity loss across ecosystems. We introduce a mathematical framework that bridges biodiversity theory and population genetics to understand the loss of naturally occurring DNA mutations with decreasing habitat. By analyzing genomic variation of 10,095 georeferenced individuals from 20 plant and animal species, we show that genome-wide diversity follows a mutations-area relationship power law with geographic area, which can predict genetic diversity loss from local population extinctions. We estimate that more than 10% of genetic diversity may already be lost for many threatened and nonthreatened species, surpassing the United Nations' post-2020 targets for genetic preservation.

Anthropogenic habitat loss and climate change (*1*) have led to the extinction of hundreds of species over the past centuries, and ~1 million more species (~25% of all known species) are at risk of extinction (*2*). Studies of species' ranges, however, have detected geographic range reductions in at least 47% of surveyed plant and animal species, likely in response to the past centuries of anthropogenic activities (*3*) [see (*4*) and table S17]. Though this loss might seem inconsequential compared with losing an entire species, this range contraction reduces genetic diversity, which dictates species' ability to adapt to new environmental conditions (*5*). The loss of geographic range can spiral into a feedback loop, where genetic diversity loss further increases the risk of species extinction (*6*, *7*).

Although genetic diversity is a key dimension of biodiversity (*8*), it has been overlooked in international conservation initiatives (*9*). Only in 2021 did the United Nations (UN) Convention of Biological Diversity propose to preserve at least 90% of all species' genetic diversity (*10*, *11*). Recent meta-analyses of animal populations with genetic marker samples have been used as proxies to quantify recent genetic changes (*12*, *13*). However, theory and scalable approaches to estimate genome-wide diversity loss across species do not yet exist, impairing prioritization and evaluation of conservation targets. Here, we introduce a framework to estimate global genetic diversity loss by bridging biodiversity theory with population genetics and by combining data on global ecosystem transformations with newly available genomic datasets.

The first studies that predicted biodiversity reductions in response to habitat loss and climate change in the 1990s and the 2000s projected species extinctions using the relationship of biodiversity with geographic area, termed the species-area relationship (SAR) (*14*) (figs. S1 to S3). In this framework, ecosystems with a larger area (A) harbor a larger number of species (S) resulting from an equilibrium among limited species dispersal, habitat heterogeneity, and colonization-extinction-speciation dynamics. Thus, the more a study area is extended, the more species are found. The SAR has been empirically shown to follow a power law, $S = A^z$. It scales consistently across continents and ecosystems (*15*), with a higher z characterizing ecosystems that are species rich and highly spatially structured. Given estimates of decreasing ecosystem area over time ($A_{t-1} > A_t$) due to human activities and climate change, Thomas *et al.* (*16*) proposed rough estimates of the percentage of species extinctions in the 21st century ranging from 15 to 37%. Though this may be an oversimplification, the SAR has become a common practical tool for policy groups, including the Intergovernmental Science-Policy Platform on Biodiversity and Ecosystem Services (IPBES) (*2*).

Akin to species richness, within-species variation can be quantitatively described by the number of genetic mutations within a species, defined here as DNA nucleotide variants that appear in individuals of a species. Although population genetics theory has long established that larger populations have higher genetic diversity (*17*), and geographic isolation between populations of the same species results in geographically separated accumulation of different mutations, there have been no attempts to describe the extent of genetic diversity loss driven by species' geographic range reduction using an analogous "mutations-area relationship" (MAR).

We suspected that such a MAR must exist given that another well-known assumption is shared between SARs and population genetics, namely that both species in ecosystems and mutations in populations are typically found in low frequencies, whereas relatively few occur at high frequencies [those that prevail through stochastic genetic drift or are favored by natural selection (*18*)]. This principle of "commonness of rarity" is well known for species and, together with limited spatial dispersal of organisms in the landscape, is a key statistical condition for the power-law SAR (when a study area is expanded, mostly rare local species are newly identified). We then quantified the rarity of mutations using 11,769,920 biallelic genetic variants of the *Arabidopsis thaliana* 1001 Genomes dataset (Fig. 1A) (*19*) by fitting several common models of species abundances (*20*) to the distribution of mutation frequencies (q), termed the site frequency spectrum in population genetics (Fig. 1B and figs. S3, S4, S12, and S13). The canonical L-shaped probability distribution ($1/q$) of this spectrum, which is expected under population-equilibrium and the absence of natural selection processes, fits these data well (Fig. 1B), although the more parameter-rich Preston's species abundance log-normal model achieved the best Akaike information criterion (AIC) value (tables S3 and S10). Despite some differences in fit, these models all showcase the similarities of abundance distributions between mutations within species and species within ecosystems, suggesting that they may also behave similarly in their relationship to geographic area (*18*, *20*).

To finally quantify how genetic diversity within a species increases with geographic area, we constructed the MAR by subsampling regions of different sizes across *A. thaliana*'s native range using more than 1000 georeferenced genomes (Fig. 1, A and C). As a metric of genetic diversity, we modeled the number of mutations in space (M, also referred to as the number of segregating sites or allelic richness) consistent with the species-centric approach of SAR, which uses species richness as the metric of biodiversity. The MAR also followed the power law relationship $M = cA^z$, where c is a

[1]Department of Plant Biology, Carnegie Institution for Science, Stanford, CA 94305, USA. [2]Department of Biology, Stanford University, Stanford, CA 94305, USA. [3]Department of Global Ecology, Carnegie Institution for Science, Stanford, CA 94305, USA. [4]Department of Zoology, University of British Columbia, Vancouver, Canada. [5]Biodiversity Research Centre, University of British Columbia, Vancouver, Canada. [6]Department of Computer Science, Stanford University, Stanford, CA 94305, USA. [7]Department of Ecology and Evolutionary Biology, University of California, Los Angeles, CA 90095, USA. [8]Center for Macroecology, Evolution and Climate, GLOBE Institute, University of Copenhagen, Copenhagen, Denmark. [9]Department of Genetics, Stanford University, Stanford, CA 94305, USA.
*Corresponding author. Email: moisesexpositoalonso@gmail.com

constant and the scaling value is z_{MAR} = 0.324 [95% confidence interval (95% CI) = 0.238 to 0.41] (Fig. 1C and tables S4 to S6). The discovered power law is robust to different methods of area quantification, subsampling effects (fully nested, outward or inward), and raster resolution (~10 to 1000 km) and is adjusted for limited sample sizes (figs. S14 to S18 and tables S7 to S9). The expected genetic diversity increase that results only from more individuals being sampled only accounts for $M \approx c\log(A) \approx cA^{z\to 0}$ [see theoretical derivation (*4*); figs. S5 and S6 and tables S1 and S2]; thus, the MAR law is attributed to fundamental evolutionary and ecological forces of population genetic drift and spatial natural selection that cause structuring of genetic diversity across populations (with a maximum $z_{MAR}\to 1$; fig. S5). MAR thus emerges in population genetics coalescent and individual-based simulations in two dimensions (figs. S6 to S8 and S10) and continuous space (fig. S9), as well as in mainland-island community assembly simulations according to the unified neutral theory of biodiversity (fig. S24).

We then asked whether MAR can predict the loss of genetic diversity due to species' range contractions. We explored several scenarios of range contraction in *A. thaliana* by removing in silico grid cells in a map representing populations (Fig. 2B). Our simulations included random local population extinction as if habitat destruction was scattered across large continents, radial expansion of an extinction front due to intense localized mortality, or local extinction in the warmest regions within a species range (*3*, *21*), among others (fig. S18). The MAR-based predictions of genetic loss, using $1-(1-A_t/A_{t-1})^{z_{MAR}}$ and assuming z_{MAR} = 0.3, conservatively followed the simulated local loss in *A. thaliana* [pseudo–coefficient of determination (R^2) = 0.87 across all simulations] (Fig. 2A and fig. S18).

To test the generality of the MAR, we searched in public nucleotide repositories for datasets of hundreds to thousands of whole-genome-sequenced individuals for the same species sampled across geographic areas within their native ranges (Table 1). In total, we identified 20 wild plant and animal species with such published resources and assembled a dataset amassing a total of 10,095 individuals of these species, with 1522 to 88,332,015 naturally occurring genome-wide mutations per species, covering a geographic area ranging from 0.03 million to 115 million km^2. Fitting the MAR for these diverse species, we recovered z_{MAR} values centered around that of *A. thaliana*, with many species overlapping in confidence intervals, and a number of outliers [mean (±SE) z_{MAR} = 0.31 (±0.038), median = 0.26, interquartile range (IQR) = ±0.15, range = 0.10 to 0.82, mean (±SE) z_{MAR} scaled (z^*_{MAR}) = 0.26 (±0.048); see Table 1, figs. S5 and S22, table S10, and (*4*)].

Table 1. MAR across diverse species. Summary statistics of the number of individuals sampled broadly per species (with the final number of samples analyzed after quality filters in parentheses), the number of naturally occurring mutations discovered through various DNA sequencing methods (see table acronyms), and the total area covered by all the samples within a species (as a convex hull of coordinates). We also report the MAR parameter z_{MAR} and its scaled version for low-sampling genomic effort per species and the percent area that needs to be kept for a species to maintain 90% of its genetic diversity calculated using z^*_{MAR}. Protected area predictions are not provided for threatened species because these have likely already lost substantial genetic diversity and require protection of their full geographic range (indicated with "–"). CA, included in the California Endangered Species Act; CR, Red List critically endangered; D, population decline reported in the Red List; GBS, genotyping by sequencing of biallelic SNP markers; GC, genotyping chip; Herb., herbaceous plant; VU, Red List vulnerable; W, whole-genome resequencing or discovery SNP calling.

Species	Group	Number of samples	Number of mutations	Area (km^2 × 10^6)	z_{MAR} (95% CI)	z^*_{MAR} (95% CI)	Minimum area$_{90\%}$ (%)
Arabidopsis thaliana	Herb.	1,135 (1,001)*	11,769,920 (W)	27.34	0.324 (0.238–0.41)	0.312 (0.305–0.32)	71–78
Arabidopsis lyrata	Herb.	108	17,813,817 (W)	2.79	0.236 (0.218–0.254)	0.151 (0.137–0.165)	50–66
Amaranthus tuberculatus	Herb.	162 (155)†	1,033,443 (W)	0.80	0.109 (0.081–0.136)	0.142 (0.136–0.149)	48–65
Eucalyptus melliodora (VU)	Tree	275	9,378 (GBS)	0.95	0.466 (0.394–0.538)	0.403 (0.398–0.407)	77–82
Yucca brevifolia (CA)	Yucca palm	290	10,695 (GBS)	NA¶	0.128# (0.109–0.147)	0.049 (0.037–0.062)	–
Mimulus guttatus	Herb. or shrub	521 (286)*	1,522 (GBS)	25.14	0.274 (0.259–0.29)	0.231 (0.221–0.241)	63–73
Panicum virgatum	Grass	732 (576)‡	33,905,044 (W)	6.29	0.232 (0.211–0.252)	0.126 (0.116–0.136)	43–63
Panicum hallii	Grass	591	45,589 (W)	2.19	0.824 (0.719–0.928)	0.814 (0.745–0.883)	88–90
Pinus contorta	Tree	929	32,449 (GC)	0.89	0.015# (0.014–0.016)	–0.061 (–0.062–0.060)	–
Pinus torreyana (CR)	Tree	242	478,238 (GBS)	NA¶	0.142# (0.142–0.142)	0.015 (0.015–0.015)	–
Populus trichocarpa	Tree	882	28,342,826 (W)	1.12	0.275 (0.218–0.332)	0.165 (0.155–0.176)	53–67
Anopheles gambiae	Mosquito	1,142	52,525,957 (W)	19.96	0.214 (0.164–0.264)	0.122 (0.111–0.132)	42–62
Acropora millepora (NT)	Coral	253	17,931,448 (W)	0.03	0.246 (0.209–0.283)	0.287 (0.28–0.294)	69–77
Drosophila melanogaster	Fly	271§	5,019 (W)	115.21	0.437 (0.397–0.477)	0.325 (0.314–0.336)	72–79
Empidonax traillii (D)	Bird	219 (199)†	349,014 (GBS, GC)	7.03	0.214 (0.174–0.254)	0.074 (0.047–0.102)	24–54
Setophaga petechia (D)	Bird	199	104,711 (GBS)	15.17	0.178 (0.134–0.223)	0.149 (0.135–0.163)	49–66
Peromyscus maniculatus	Mammal	80 (78)†	14,076 (GBS)	22.61	0.488 (0.264–0.713)	0.683 (0.615–0.751)	86–88
Dicerorhinus sumatrensis (CR)	Mammal	16	8,870,513 (W)	NA¶	0.412# (0.369–0.456)	0.127 (0.11–0.144)	–
Canis lupus	Mammal	349 (230)‡	1,517,226 (W)	19.10	0.256 (0.232–0.28)	0.184 (0.175–0.193)	56–70
Homo sapiens	Mammal	2,504	88,332,015 (W)	80.76	0.431# (0.347–0.514)	0.281 (0.23–0.332)	–

*Only individuals in the native range were used for the analyses. †Only individuals with available coordinates or matching IDs were used for the analyses. ‡Only natural populations were used, excluding breeds, landraces, and cultivars. §Numbers indicate pools of flies used for pool sequencing rather than individuals. ¶Not applicable. Area was not reported for species with unknown locations or where two or fewer populations were sampled. #Values excluded from global averages were used for conservation applications owing to uncertain estimates, suboptimal genomic data type, or because estimates should not be applied for conservation (i.e., humans or nearly extinct Sumatran rhinoceros) [see (*4*)].

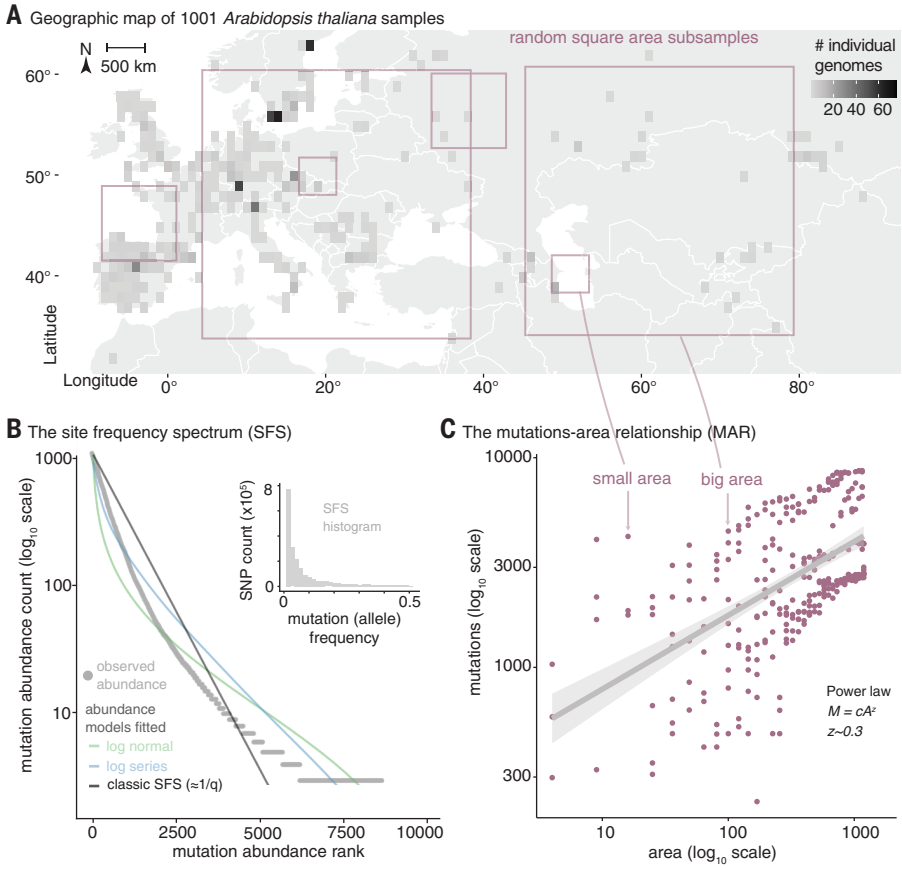

Fig. 1. Mutations across populations fit models of species abundance distributions and a power law with species range area. (**A**) Density of individual genomes projected in a 1°-by-1° latitude-longitude map of Eurasia and exemplary subsample areas of different sizes. (**B**) Distribution of mutation [single-nucleotide polymorphism (SNP)] frequencies in 1001 *A. thaliana* plants using a site frequency spectrum (SFS) histogram (gray inset) and a Whittaker's rank abundance curve plot. Also shown are the fitted models of common species abundance functions in *A. thaliana* using a dataset random sample of 10,000 mutations that are also used in (C). (**C**) The MAR in log-log space built from 340 random square subsamples (red dots) of different areas of increasing size within *A. thaliana*'s geographic range along with the number of mutations discovered within each area subset.

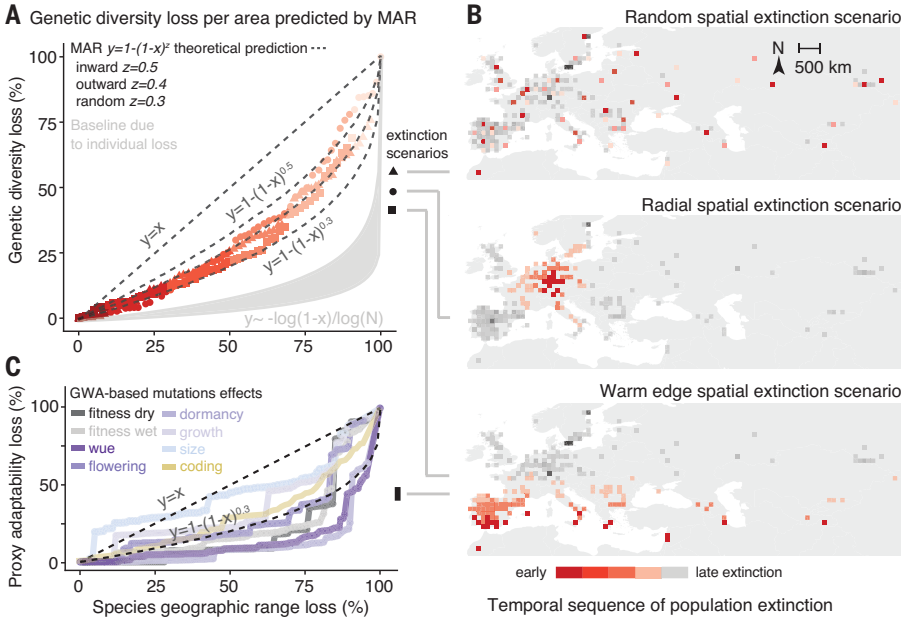

Fig. 2. The power law of genetic diversity loss with range area loss. (**A**) Percentage of loss of total genetic diversity in *A. thaliana* from several stochastic simulations (red) of local extinction in (B) and theoretical model projections of genetic diversity loss using the MAR (dashed lines). The expectation for genetic diversity loss based only on individuals is in gray [using starting populations of $N = 10^4$ to 10^9; see derivation (4)]. (**B**) Illustrated example of several possible range contractions simulated by progressively removing grid cells across the map of Eurasia (red and gray boxes) after different hypothesized spatial extinction patterns. (**C**) A metric of adaptive capacity loss during warm edge extinction in (B) using GWA to estimate effects of mutation on fitness in different rainfall conditions, water-use efficiency (wue), flowering time, seed dormancy, plant growth rate, and plant size. Plotted are the fraction loss of the summed squared effects ($\sum a^2$) of 10,000 mutations from the top 1% tails of effects. Also plotted is the fraction of protein-coding alleles lost (nonsynonymous, stop codon loss or gain, and frameshift mutations; yellow line).

Although we expect species-specific traits related to dispersibility or gene flow to affect z_{MAR} (e.g., migration rate and environmental selection in population genetic simulations significantly influence z_{MAR}; table S2), no significant association was found in an analysis of variance (ANOVA) between z_{MAR} and different traits, mating systems, home continents, and so on for the 20 species analyzed (tables S12 to S13). There may be too few species with large population genomic data to find such a signal (Table 1 and tables S12 and S13). For conservation purposes, an average z_{MAR} ~ 0.3 (IQR = ±0.15; Table 1 and table S11) could be predictive of large-scale trends of genetic diversity loss in many range-reduced species that lack genomic information. Further, although species will naturally have different starting levels of total genetic diversity before range reductions due to, for instance, genome size, structure, or mating system differences (*17*), the application of z_{MAR} will provide relative estimates of genetic diversity loss. For instance, assuming z_{MAR} ~ 0.3, we would predict that an area reduction of ~50% creates a loss of ~20% of genetic diversity relative to the total genetic diversity of a given species.

Finally, we used MAR to estimate the average global genetic diversity loss caused by pre–21st century land transformations. Although accurate species-specific geographic area reduction data in the past centuries are scarce, we leveraged global land cover transformations from primary ecosystems to urban or cropland systems (*2*, *22*) (tables S14 to S16). Using the average z^*_{MAR} and several global averages of Earth's land and coastal transformations for present day [38% global area transformation from (*22*), 34% from (*2*), and 43 to 50% from (*23*)], we estimate a 10 to 16% global genetic diversity loss, on average, across species (Fig. 3, A and B). Although these estimates may approximate central values across species in an ecosystem, we expect a substantial variation in the extent of loss across species, ranging theoretically from 0 to 100% (Fig. 3, fig. S26, and table S18), and expect that species extinction (100% area and genetic diversity lost) will substantially contribute to ecosystem-wide genetic diversity losses (figs. S25 and S27). One cause of this variation of losses across species is the heterogeneity in land-cover transformations across ecosystems; for example, more-pristine high-altitude systems have only lost 0.3% of their area, whereas highly managed temperate forests and woodlands have lost 67% (Fig. 3B and tables S14 and S15).

Another cause for the variability in genetic loss among species (even within the same ecosystem) may be their differential geographic ranges and abundances, life histories, tolerance to transformed habitats, or species-specific threats. We gathered data from species red-listed by the International Union for Conservation of Nature (IUCN) (*24*), which evaluates recent population or geographic range area reduction over ±10 years or ±3 generations to place assessed species in different threat categories using several criteria and thresholds (*24*). Assuming that the average z^*_{MAR} can capture general patterns, we translate criterion A2-4c thresholds, which document geographic range loss, into genetic diversity loss [Fig. 3C and table S17; see (*4*)]. "Vulnerable" species, having lost at least 30% of their geographic distribution, may have experienced >9% of genetic diversity loss; "endangered" species, which have lost more than 50% of their geographic distribution, should have incurred >16% of genetic diversity loss; and "critically endangered" species, with more than 80% area reduction, likely suffered >33% of genetic diversity loss (Fig. 3C). This showcases that even species at no imminent risk of extinction (e.g., least concern, near threatened, vulnerable), such as most species for which population genomic data exists, may already be losing genetic diversity (Fig. 3A).

If future habitat losses are not prevented, genetic diversity will continue eroding. In support of this claim, habitat projections to 2070 of 19,365 threatened and nonthreatened mammal, bird, and amphibian species from the Map of Life (*25*) show an average 2% genetic diversity decline (Fig. 3D), and a total of 1843 species (3%) are projected to

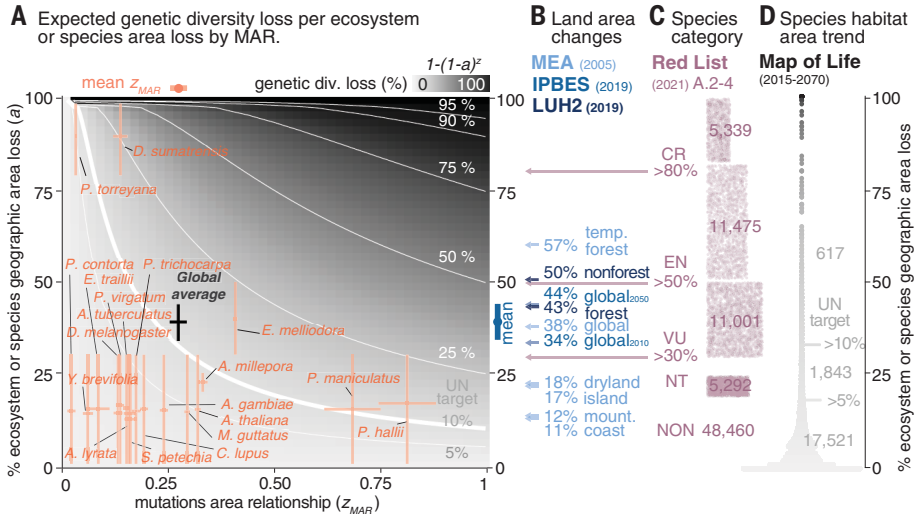

Fig. 3. The parameter space of genetic diversity loss mapping before 21st century ecosystem transformations and species threat categories against possible values of the MAR. (**A**) Possible values of two key parameters, the MAR scaling parameter (z_{MAR}) and percentage of area reduction (*a*) of a species geographic range (as a proxy of entire ecosystem transformation). The theoretical percentage of genetic diversity loss is represented as filled gray color, with isolines in white. Estimates of z^*_{MAR} from Table 1 per species are in orange with their 95% CIs (see fig. S23 for the unscaled z_{MAR}). Past area losses for these species are unknown. As a proxy with much uncertainty, species are plotted based on their IUCN Red List status, which under criterion A2-4 can be used to determine the minimum range area decline (C). The global average is calculated with the average z^*_{MAR} across species and the total percentage of Earth transformed as published by IPBES. (**B**) Percentages of transformed ecosystem areas from the Millennium Ecosystem Assessment (MEA) (table S14) are represented by light blue arrows, from IPBES (*2*) for 2010 and 2050 by dark blue arrows (table S15), and from the Land Use Harmonization 2 (LUH2) dataset (*23*) by deep blue arrows (table S16). (**C**) Lilac-colored arrows indicate the minimum value of geographic area loss under criteria A2-4c to be classified in each category of the IUCN Red List guidelines (*24*): near threatened (NT), vulnerable (VU), endangered (EN), critically endangered (CR), and nonthreatened (NON). The dotplots with pseudo-random numbers within the established thresholds represent plant, mammal, bird, and amphibian species categorized using criteria A2-4 (table S17). (**D**) Projected area loss from 2015 to 2070 by the Map of Life (mol.org) for mammal, bird, and amphibian species (*25*) (data are not available for plants). Color scale is the same as in (A) and indicates genetic diversity loss assuming the global average z^*_{MAR}.

lose at least 5% genetic diversity in the next decades.

Once lost, the recovery of genetic diversity through natural mutagenesis is extremely slow (*26*), especially for positive mutations that contribute to adaptation. Simulating a species undergoing only a 5 to 10% reduction in area, it would take at least ≈140 to 520 generations to recover its original genetic diversity (2100 to 7800 years for a fast-growing tree or medium–life span mammal of 15-year generation length); although for most simulations, recovery virtually never happened over millennia (fig. S11).

The ultimate challenge is to understand how genetic diversity loss relates to loss of adaptive capacity of a species. To this end, we leveraged the extensive knowledge of the effect of mutations in ecologically relevant traits in *A. thaliana* from genome-wide associations (GWAs). We again conducted spatial warm-edge extinction simulations, this time tracking metrics of adaptive capacity, including the total sum of effects estimated from GWA of remaining mutations ($\sum_i a^2{}_i$ for i = 1...10,000 variants of putative a_i effect), the additive genetic variance [$Va = \sum_i p_i(1 - p_i)a_i{}^2$, which accounts for each variant's population frequency p_i], and the loss of nonsynonymous mutations (Fig. 2C and figs. S19 to S21). Although determining the effect of mutations through GWA is technically challenging even in model species (*27*), and variants may even be either deleterious or advantageous depending on genomic backgrounds (*28*) or environments (*29*), our analyses suggest that putatively functional mutations may be more slowly lost as area is lost ($z < 0.3$; Fig. 2C) than neutral genetic diversity (Fig. 2A and table S9). Indeed, the additive variance Va parameter, often equated to the rate of adaptation, appears rather stable (*30*) until just before the extinction event when it sharply collapses (fig. S21; for simulations that replicate this pattern see fig. S9). This is analogous to the famous "rivet popper" metaphor where ecosystem structure and function may suddenly collapse as species are inadvertently lost (*31*). Projections of the MAR using genome-wide variation thus may crucially serve as an early conservation tool in nonthreatened species (*32*), before species reach accelerating collapsing extinction dynamics—an acceleration that we expect to be even more dramatic owing to increased drift and accumulation of deleterious mutations of small critically endangered populations (*6*).

To achieve the recently proposed UN target to protect "at least 90% of genetic diversity within all species" (*11*), it will be necessary to aggressively protect as many populations as possible for each species. Here, we have discovered the existence of a MAR and provided a mathematical framework to forecast genetic diversity loss with shrinking geographic species ranges. The MAR contrasts with existing studies on the risk of losing entire species by focusing on quantifying the magnitude and dynamics of genetic diversity loss that is likely ongoing in most species. This framework demonstrates that even with conservative estimates, substantial area protection will be needed to meet the UN Sustainable Development Goals. For vulnerable or endangered species, we have likely already failed.

REFERENCES AND NOTES

1. S. Díaz *et al*., *Science* **366**, eaax3100 (2019).
2. Intergovernmental Science-Policy Platform on Biodiversity and Ecosystem Services (IPBES), *The Global Assessment Report on Biodiversity and Ecosystem Services*, E. S. Brondizio, J. Settele, S. Diaz, H. T. Ngo, Eds. (IPBES Secretariat, Bonn, 2019).
3. J. J. Wiens, *PLOS Biol.* **14**, e2001104 (2016).
4. See supplementary materials and methods.
5. C. Parmesan, *Annu. Rev. Ecol. Evol. Syst.* **37**, 637–669 (2006).
6. M. Lynch, J. Conery, R. Burger, *Am. Nat.* **146**, 489–518 (1995).
7. D. Spielman, B. W. Brook, R. Frankham, *Proc. Natl. Acad. Sci. U.S.A.* **101**, 15261–15264 (2004).
8. W. Steffen *et al*., *Science* **347**, 1259855 (2015).
9. L. Laikre *et al*., *Science* **367**, 1083–1085 (2020).
10. S. Díaz *et al*., *Science* **370**, 411–413 (2020).
11. Convention on Biological Diversity (CBD), "First draft of the post-2020 Global Biodiversity Framework" (CBD/WG2020/3/3, United Nations Environment Programme, 2021); https://www.cbd.int/doc/c/abb5/591f/2e46096d3f0330b08ce87a45/wg2020-03-03-en.pdf.
12. D. M. Leigh, A. P. Hendry, E. Vázquez-Domínguez, V. L. Friesen, *Evol. Appl.* **12**, 1505–1512 (2019).
13. K. L. Millette *et al*., *Ecol. Lett.* **23**, 55–67 (2020).
14. O. Arrhenius, *J. Ecol.* **9**, 95–99 (1921).
15. D. Storch, P. Keil, W. Jetz, *Nature* **488**, 78–81 (2012).
16. C. D. Thomas *et al*., *Nature* **427**, 145–148 (2004).
17. V. Buffalo, *eLife* **10**, e67509 (2021).
18. R. A. Fisher, *Proc. R. Soc. Edinb.* **50**, 204–219 (1931).
19. 1001 Genomes Consortium, *Cell* **166**, 481–491 (2016).
20. F. W. Preston, *Ecology* **43**, 185 (1962).
21. A. Hampe, R. J. Petit, *Ecol. Lett.* **8**, 461–467 (2005).
22. Millennium Ecosystem Assessment, "Ecosystems and human well-being: Biodiversity synthesis" (World Resources Institute, 2005); https://www.millenniumassessment.org/en/index.html.
23. G. C. Hurtt *et al*., *Geosci. Model Dev.* **13**, 5425–5464 (2020).
24. International Union for Conservation of Nature (IUCN), "Guidelines for using the IUCN Red List categories and criteria," version 15 (IUCN, 2022); https://www.iucnredlist.org/resources/redlistguidelines.
25. R. P. Powers, W. Jetz, *Nat. Clim. Chang.* **9**, 323–329 (2019).
26. D. L. Halligan, P. D. Keightley, *Annu. Rev. Ecol. Evol. Syst.* **40**, 151–172 (2009).
27. M. V. Rockman, *Evolution* **66**, 1–17 (2012).
28. M. J. Harms, J. W. Thornton, *Nat. Rev. Genet.* **14**, 559–571 (2013).
29. M. Exposito-Alonso, H. A. Burbano, O. Bossdorf, R. Nielsen, D. Weigel, 500 Genomes Field Experiment Team, *Nature* **573**, 126–129 (2019).
30. H. R. Taft, D. A. Roff, *Conserv. Genet.* **13**, 333–342 (2012).
31. P. Ehrlich, B. Walker, *Bioscience* **48**, 387 (1998).
32. M. Kardos *et al*., *Proc. Natl. Acad. Sci. U.S.A.* **118**, e2104642118 (2021).
33. M. Exposito-Alonso, Scripts to build the mutations area relationship. Zenodo (2022); https://doi.org/10.5281/zenodo.6408624.

ACKNOWLEDGMENTS

We are grateful to the openness of many researchers who make genomic data publicly available and this research possible: the 1001 *Arabidopsis* Genomes Consortium, the *Anopheles gambiae* 1000 Genomes Consortium, the 1000 (Human) Genome Consortium, the European Drosophila Evolution over Space and Time (DEST) Consortium, MacLachlan *et al*., Fuller *et al*., Ruegg *et al*., Kingsley *et al*., Schweizer *et al*., and Royer *et al*. In addition, we are grateful to all the authors who shared intermediate genome variant files: S. Mamidi, J. Lovell, D. Jacobson, M. Shah, J. Kreiner, K. Lucek, Y. Willi, J. D. Palacio Mejia, J. Borevitz, M. Supple, M. Vallejo-Marin, N. Dussex, L. Di Santo, and J. Hamilton. We thank W. Jetz for fruitful discussions and for sharing range data from Map of Life (mol.org). We thank J. Wiens, S. Rhee, D. Weigel, E. Armstrong, M. Kardos, D. Petrov, R. Colwell, R. Nielsen, A. Michalak, S. Hoban, J. Pritchard, T. Fukami, and members of the Moi and Mordecai labs for comments, discussion, or references. **Funding:** M.E.-A. and this research are supported by the Office of the Director of the National Institutes of Health's Early Investigator Award (1DP5OD029506-01); by the U.S. Department of Energy, Office of Biological and Environmental Research (DE-SC0021286); and by the Carnegie Institution for Science. J.P.S. is supported by an NIH training grant (5T32HG000044-23), and S.T.A by the National Institute of General Medical Sciences center of the NIH (T32GM007276). S.H. and C.L.W. are supported by Stanford's Center for Computational, Evolutionary, and Human Genomics. P.L.M.L. is supported by a Human Frontier Science Program Long-Term Fellowship (LT000330/2019-L). M.R. is supported by the NSF Postdoctoral Research Fellowships in Biology program (2109868). L.L. and L.G. are supported by NSF's Graduate Research Fellowship Program. Computational analyses were done on the high-performance computing clusters *Memex*, *Calc*, and *MoiNode* supported by the Carnegie Institution for Science. **Author contributions:** After the first author, authors are listed in alphabetical order. M.E.-A. conceived and led the project. M.E.-A., J.P.S., M.R., S.H., L.G., L.C., L.L., S.E.T.A., V.P., E.Z., P.L.M.L., C.C.K., T.R.B., and C.L.W. conducted research; all authors interpreted the results and wrote the manuscript. **Competing interests:** The authors declare no competing financial interests. **Data and materials availability:** The analyzed datasets are publicly available (see supplementary materials for data links). Code is available at Github (https://github.com/moiexpositoalonsolab/mar) and Zenodo (*33*).

SUPPLEMENTARY MATERIALS

science.org/doi/10.1126/science.abn5642
Materials and Methods
Figs. S1 to S27
Tables S1 to S18
References (*34*–*90*)
MDAR Reproducibility Checklist

View/request a protocol for this paper from *Bio-protocol*.

Submitted 6 December 2021; accepted 8 August 2022
10.1126/science.abn5642

Science

Genetic diversity loss in the Anthropocene

Moises Exposito-AlonsoTom R. BookerLucas CzechLauren GillespieShannon HateleyChristopher C. KyriazisPatricia L. M. LangLaura LeventhalDavid Nogues-BravoVeronica PagowskiMegan RuffleyJeffrey P. SpenceSebastian E. Toro AranaClemens L. WeißErin Zess

Science, 377 (6613), • DOI: 10.1126/science.abn5642

Declining genetic diversity

Habitat loss is one of the major drivers of species extinctions and declines of species richness at local scales. Smaller areas of remnant habitat also harbor smaller populations and lower genetic diversity, which may limit potential adaptation to environmental change. Exposito-Alonso *et al*. developed a framework to predict decreases in naturally occurring mutations, and thus genetic diversity, with habitat loss (see the Perspective by Ruegg and Turbek). Georeferenced genomic data from across the native ranges of the small mustard plant *Arabidopsis thaliana* and 20 other species suggest that the mutation-area relationship follows a power law. This relationship predicts that many species have already experienced substantial genetic diversity loss. —BEL

Science (ISSN) is published by the American Association for the Advancement of Science. 1200 New York Avenue NW, Washington, DC 20005. The title *Science* is a registered trademark of AAAS.